

A Study of Position Control and Design for Microelectrostatic Mechanical Actuator

Won Seok Choi[†], Tea Young Jee[†], Kun Nyun Kim^{*}, Hyo Derk Park^{**} and Hoon Heo^{††}

미세 작동기의 설계 및 위치 제어에 관한 연구

최원석[†] · 지태영[†] · 김건년^{*} · 박효덕^{**} · 허훈^{††}

Key Words: *electrostatic force* (정전기력), *Mems actuator* (미소 작동기), *pull-in voltage* (풀인 전압), *position control* (위치 제어), *PID controller* (PID 제어기).

Abstract

Microactuator is frequently used in some optical or electrical applications such as light modulators and spatial scanner devices. When microactuator is implemented, it should be operated at accurate positions proportional to input voltage. Therefore in order to obtain rapid responses and reduced errors, a position control technique is used. In the paper, design procedure for the mems actuator and a typical PID controller is adapted to improve performance of microactuator as well. Also electrostatic force for the torsional microactuator is calculated via well-known Hornbeck's method.

Nomenclature

W_p : width of mainplate
 L_p : length of mainplate
 t_p, t_b : thickness of plate, beam
 W_b : width of suspension beam
 L_b : length of suspension beam
 D : initial gap of two plates
 G : shear modules of silicon
 E : Young's modules of silicon
 I_θ : inertia of mainplate
 K_θ : inertia of suspension beam

T : applied torque
 P : applied load
 I_b : inertia of suspension beam
 ε : dielectric constant
 b : damping coefficient
 V : applied voltage

1. Introduction

Recently, the electrostatic actuators have gained a lot of attention for various MEMS device. As a result of the development of microfabrication technology, micromechanical structures and microsensors have been used widely. The dynamic performances such as response time and sensitivity of a microactuator are better than those of a conventional actuator because of the small size and weight [1]. However, the applications of microactuators are limited by their loading capacity, strength,

[†] 고려대학교 제어계측공학과 대학원

E-mail : wraith@cie.korea.ac.kr

TEL : (02)3290-3995 FAX : (02)929-7808

^{*} 전자부품 연구원 (KETI) 나노메카트로닉스 책임 연구원

^{**} 전자부품 연구원 (KETI) 나노메카트로닉스 센터장

^{††} 고려대학교 제어계측공학과 교수

and traveling range. Presently, microactuators are primarily applied in transmitting such physical quantities as electromagnetic, acoustic, and light energy, instead of force [2]~[4]. Since the microtorsional actuator is primarily performing out of plane angular motion, it is the most common device for the above applications. For example, torsional microactuators are applied in optical switches, light modulators, projection television optical choppers, optical shutters, bar code readers and light positioners.

The goal of the study is to develop a controller of microelectrostatic torsional actuator (META) and improve its performance. A typical META usually consists of the following mechanical components: suspensions, a mirror plate, and electrodes, as shown in [Fig. 1]. A closed-loop feedback-control system that drastically improves the dynamic response, settling time, and external disturbance rejection characteristics of an electrostatic actuator is demonstrated. A proportional-derivative-integral controller is used to increase position accuracy of the micromirror. ($W_p = 612 \mu m$, $L_p = 400 \mu m$, $t_p, t_b = 10 \mu m$, $W_b = 16 \mu m$, $L_b = 25 \mu m$, $D = 8 \mu m$)

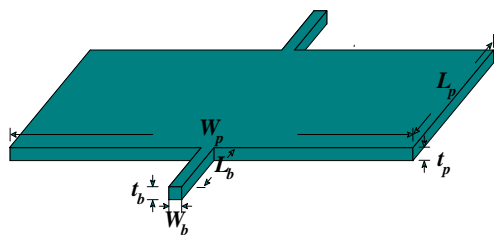


[Fig. 1] A schematic view of rectangular electrostatic torsional actuator

2. System Analysis

2.1 Structure analysis

2.1.1 Static analysis

The determination of the stress in noncircular members subjected to a torsional loading is beyond the scope of this paper. However, the

result obtained from the mathematical theory of elasticity for straight bar with a uniform rectangular cross section will be indicated here for convenience.

It is well known that the maximum shearing stress τ_{max} occurs along the center of the wider face of the bar and is equal to

$$\tau_{max} = \frac{T}{c_1 W_b t_b^2} \quad [2 - 1]$$

the angle of twist φ , on the other hand, may be expressed as

$$\varphi = \frac{TL_b}{c_2 W_b t_b^3 G} \quad [2 - 2]$$

The coefficients c_1 and c_2 depend only upon the ratio W_b/t_b and here, $c_1 = 0.231$ $c_2 = 0.1958$ for a number of values of the ratio. Note that eqn. [2 - 1] and [2 - 2] are valid only within the elastic range [5].

$\tau_{max} = 5.1389e+3 \ll G$, $\varphi = 3.1093e-8 \text{ }^\circ \approx 0$ according to these parameters are optimal and structure is settled

■ Deflection of suspension beam

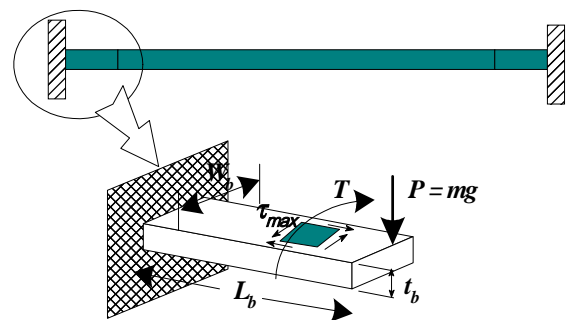


[Fig. 2] Suspension beam

Maximum deflection d_{max} of suspension beam is :

$$d_{max} = -\frac{PL_b^3}{3EI_b} \quad [2 - 3]$$

$d_{max} = 3.21e-9 m$ so d_{max} is ignored.

2.1.2 Dynamic analysis

As the results that observed in the previous chapter, the model is regarded as a rigid body. Accordingly no modal analysis for a flexible model is carried out in the study. However the first resonance frequency ($\omega_n = 39.472\text{kHz}$) of a microactuator by useful FEM (Finite-elements model) is obtained via ANSYS 6.1 and approximate the system can be regarded as SISO (Single Input Single Output) system.

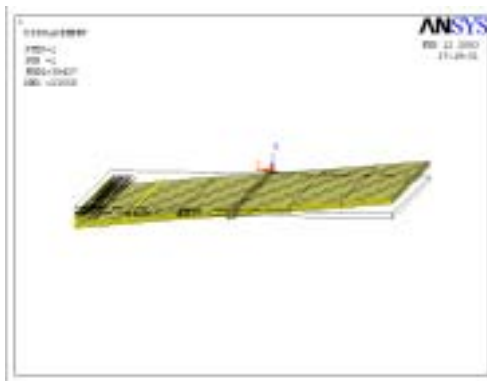


[Fig. 3] First mode shape & natural freq. ω_n

■ First order Linear Equation

$$I_\theta \ddot{\theta} + b \dot{\theta} + k_\theta \theta = T \quad [2 - 4]$$

The parameter of the torsional stiffness of the beam and the moment of inertia can be calculated from the design parameter [6]. Also the damping coefficient can only be obtained by experimental data. Here, we assign a constant for using ANSYS 6.1

2.2 Electrostatic Force analysis

An electrostatic actuation is the most frequently applied principle combining versatility and simple technology. All electrostatic devices operate on the principle that opposite charges attract. There are multiple ways in which this phenomenon is implemented in microactuators.

■ Electrostatic Energy and Force

- Storage charge :

$$Q = CV \quad [2 - 5]$$

- Electrostatic energy :

$$W = \frac{1}{2} CV^2 \quad [2 - 6]$$

- Electrostatic force :

$$F_E = -\frac{\partial W}{\partial x} \quad [2 - 7]$$

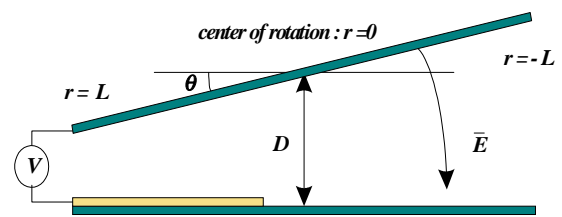


[Fig. 4] Schematic side view of the torsional actuator

The mainplate of the microactuator is considered to be a tiltable rigid body. Hence, the only degree of freedom to take into account is the angle of torsion θ . The differential force acting on a segment of the actuation electrode is equal to that of a differential parallel plate capacitor with width W_P and infinitesimal length dr :

$$dF = \frac{1}{2} \epsilon V^2 \frac{W_P dr}{(D - r \sin \theta)^2} \quad [2 - 8]$$

In the notation of Kirchhoffian network variables, the quantity conjugate to the generalized force across variable $d\theta/dt$ angular velocity of torsion is the torque T which play the role of the generalized flow through quantity

$$T = \int_0^L r dF = \frac{1}{2} \epsilon V^2 \int_0^L \frac{r}{(D - r \sin \theta)^2} dr \quad [2 - 9]$$

Integration over the effective electrode area on the mainplate yields

$$T = \frac{1}{2} \varepsilon \frac{V^2 L^2}{D^2} W_P \frac{1}{\gamma^2} \left(\frac{\gamma}{1-\gamma} + \log(1-\gamma) \right) \quad [2-10]$$

where normalized angle γ :

$$\gamma = \frac{\sin \theta}{\sin \theta_0} \approx \frac{\theta}{\theta_0} \quad [2-11]$$

and the maximum torsional angle θ_0 :

$$\theta_0 = \arcsin \frac{D}{L} \approx \frac{D}{L} \quad [2-12]$$

The capacitance can be calculated from the electric field distribution

$$E(r) = \frac{V}{(D - r \sin \theta)} \quad [2-13]$$

according to

$$Q = \int_{\text{electrode}} \varepsilon \bar{E} d\bar{a} = \int_0^L \frac{r}{(D - r \sin \theta)^2} dr \quad [2-14]$$

hence

$$C = \frac{Q}{V} = \varepsilon \frac{W_P L}{D} \log(1-\gamma) \quad [2-15]$$

If the actuator is driven with charges control variable, then $\frac{Q}{C}$ is substituted for V in eqn. [2-6], yielding :

$$T = \frac{1}{2} \frac{Q^2}{\varepsilon W_P} \frac{1}{(\log(1-\gamma))^2} \left(\frac{\gamma}{1-\gamma} + \log(1-\gamma) \right) \quad [2-16]$$

2.3 Pull-In voltage and Pull-In angle analysis

One of important parameters of electrostatic microactuators is the pull-in voltage. In static equilibrium, the electrostatic force/torque and the mechanical force/torque are equal, resulting in a stable condition for the actuator. As the voltage is increased, the electrostatic force/torque increases and eventually overcomes the mechanical force/torque, resulting in instability or collapse condition, where a contact between the two plates is formed. Analytical solution of

Hornbeck's [7] method and FEM (finite elements model) approach by ANSYS 6.1 are compared [8].

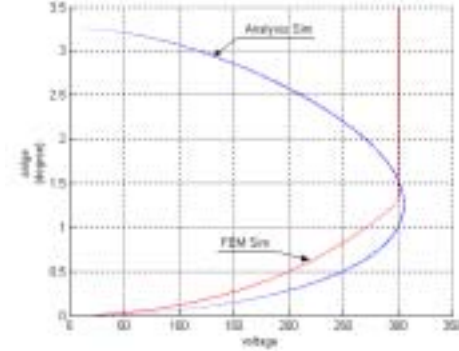


[Fig. 5] Analysis vs. FEM Simulation

The pull-in voltage for the model is about 300 V by analytical and FEM method. The difference between two methods is small. In the experiment the voltage less 300 V is applied.

3. Controller Design

3.1 Derivation of characteristic equation

■ Linear System

From eqn. [2-4] we represent state-space equation form.

$$\dot{\mathbf{x}}(t) = \mathbf{A} \mathbf{x}(t) + \mathbf{B} \mathbf{u}(t) \quad [3-1]$$

$\mathbf{x}(t)$: state variables vector in time domain

\mathbf{A} : system matrix

\mathbf{B} : input matrix

$\mathbf{u}(t)$: control input in time domain

By eqn. [2-10], the state equation can be arranged as

$$\begin{aligned} \begin{bmatrix} \dot{\theta} \\ \ddot{\theta} \end{bmatrix} &= \begin{bmatrix} 0 & 1 \\ -\frac{k_\theta}{I_\theta} & -\frac{b}{I_\theta} \end{bmatrix} \begin{bmatrix} \theta \\ \dot{\theta} \end{bmatrix} + \begin{bmatrix} 0 \\ \frac{1}{I_\theta} \end{bmatrix} T \\ &= \begin{bmatrix} 0 & 1 \\ -\frac{k_\theta}{I_\theta} & -\frac{b}{I_\theta} \end{bmatrix} \begin{bmatrix} \theta \\ \dot{\theta} \end{bmatrix} + \begin{bmatrix} 0 \\ \frac{\varepsilon L^2}{2I_\theta D^2} w \frac{1}{\gamma^2} \left(\frac{\gamma}{1-\gamma} + \log(1-\gamma) \right) \right] V^2 \end{aligned} \quad [3-2]$$

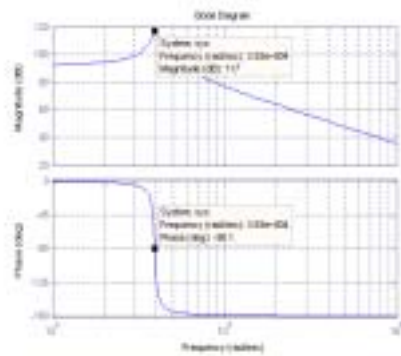


[Fig. 6] Bode plot of torsional actuator

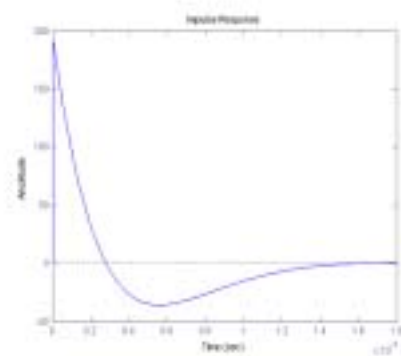


[Fig. 8] Impulse response by Feedback

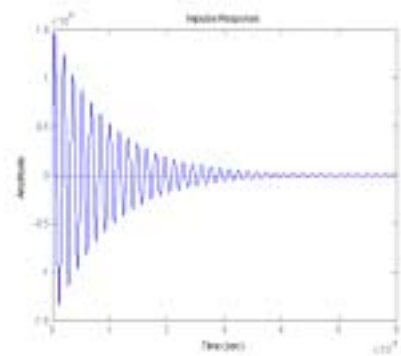


[Fig. 7] Impulse response of uncompensated system

Due to the small size and high natural frequency of designed actuator, it is characterized of large response short settling time.

3.2 PID controller design

From Eqn [3 - 2] we obtain general second order transfer function $G(s)$

$$G(s) = \frac{\omega_n^2}{s^2 + 2\zeta\omega_n s + \omega_n^2} \quad [3 - 3]$$

and we design $K(s)$:

$$K(s) = K_p + \frac{K_i}{s} + K_d s \quad [3 - 4]$$

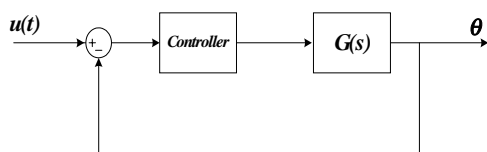


[Fig. 7] Feedback block diagram

[Table 1] System response normal vs Compensated

	Magnitude	t_s
Uncontrolled	1.5×10^9	6×10^{-3}
Compensated	200	1.8×10^{-4}

As a result of improvement with PID controller, a tremendously decreased response in magnitude and shortend response time as well.

3.3 Virtual model simulation

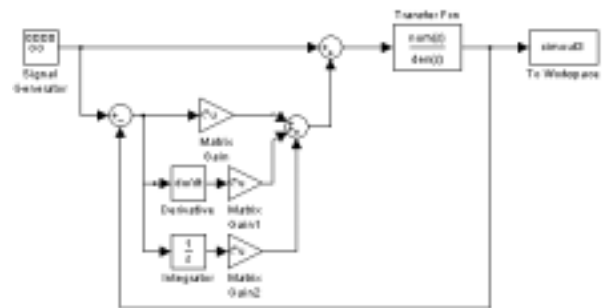


[Fig. 9] Block diagram of virtual model

For physical torsional actuator, investigation of the response along the induced voltage of pulse type will be carried out in the experiment. An applied plant model is biased according to one side electrode situation. If positive voltage of signal generator is electrostatic force that pull up one side of model, then negative voltage is reversed. At this time, we observe overshoot, oscillation and compensate system response by controller.

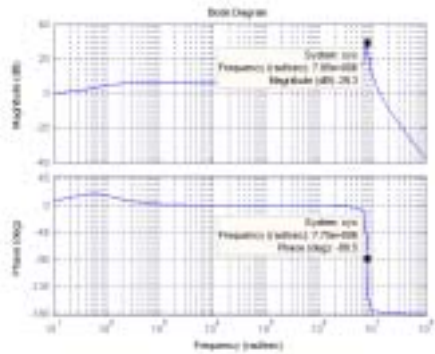


[Fig. 10] Bode plot of compensated system

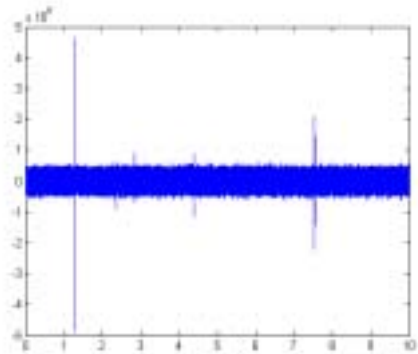


[Fig. 11] Uncompensated system input plot

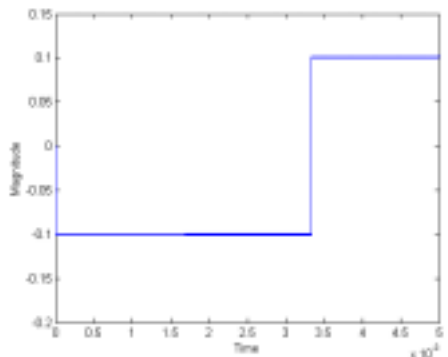


[Fig. 12] Observe system_PID controlled

4. Conclusions

Optimal parameter values for the stable microactuator are obtained via structural analysis. Micro torsional actuator using conventional PID controller shows drastic improvement of its performance and reveals to be proper as actuator. Actuator design procedure proved to be successful to realize it. Currently it is fabricated and experiment is being carried on.

Acknowledgement

This work was supported by MOCIE

Reference

- [1] W. Trimmer, *Micromechanical System*, The Third Toyota Conference, 1989, pp. 1-15.
- [2] H. Toshiyoshi, H. Fujita, *Electrostatic micro torsion mirrors for an optical switch matrix*, *Journal of Microelectromechanical System* 5, 1996 231~237.
- [3] D. Chauvel, N. Haese, P.A. Rolland, D. Collard, H. Fujita, *A micro-machined microwave antenna integrated with its electrostatic spatial scanning*, *The Tenth Annual International Workshop on Microelectromechanical System*, 1997, pp. 84~89.
- [4] S.S. Lee, R.P. Ried, R.M. White, *Piezoelectric cantilever microphone and micro speaker*, *Journal of Microelectromechanical System* 5 (4) (1996) 238~242.
- [5] Ferdinand P. Beer, E. Russell Johnston Jr. *Vector Mechanics for Engineers static* : McGraw-Hill 2th.
- [6] S. P. Timoshenko and I. N. Goodier, *Theory of Elasticity*. New York : McGraw-Hill, 1970
- [7] L. J. Hornbeck, "Deformable-mirror spatial light modulators," in *SPIE critical Review Series-Spatial Light Modulators and Applications III*. 1989, vol. 1150, pp 86-102
- [8] O. Degani, E. Socher, A. Lipson " Pull-In Study of an Electrostatic Torsion Microactuator", *Journal of Microelectromechanical Systems* 1998 Vol 7, No 4, pp 373-378.